Source Forensics of Black Carbon Aerosols from China

ARTICLE *in* ENVIRONMENTAL SCIENCE & TECHNOLOGY · JULY 2013

Impact Factor: 5.33 · DOI: 10.1021/es401599r · Source: PubMed

12 AUTHORS, INCLUDING:

August Andersson
Stockholm University
58 PUBLICATIONS **797** CITATIONS
SEE PROFILE

Meinan Shi
China University of Geosciences (Beijing)
4 PUBLICATIONS **29** CITATIONS
SEE PROFILE

Zifeng Lu
Argonne National Laboratory
22 PUBLICATIONS **400** CITATIONS
SEE PROFILE

Ke Du
The University of Calgary
33 PUBLICATIONS **257** CITATIONS
SEE PROFILE

Environmental Science & Technology

Article

pubs.acs.org/est

Source Forensics of Black Carbon Aerosols from China

Bing Chen,[†,‡,○] August Andersson,[§] Meehye Lee,[∥] Elena N. Kirillova,[§] Qianfen Xiao,[⊥] Martin Krusa,[§] Meinan Shi,[#] Ke Hu,[#] Zifeng Lu,[▽] David G. Streets,[▽] Ke Du,[*,†] and Örjan Gustafsson[*,§]

[†]Institute of Urban Environment, Chinese Academy of Sciences, Xiamen 361021, China

[‡]Associate Unit CSIC-University of Huelva "Atmospheric Pollution", University of Huelva, E21071 Huelva, Spain

[§]Department of Applied Environmental Science and the Bert Bolin Centre for Climate Research, Stockholm University, 10691 Stockholm, Sweden

[∥]Department of Earth and Environmental Sciences, Korea University, Seoul 136-701, South Korea

[⊥]School of Environmental Science and Technology, Tongji University, Shanghai 200092, China

[#]School of Marine Science, China University of Geosciences, Beijing 100038, China

[▽]Decision and Information Sciences Division, Argonne National Laboratory, Argonne, Illinois 60439, United States

Supporting Information

ABSTRACT: The limited understanding of black carbon (BC) aerosol emissions from incomplete combustion causes a poorly constrained anthropogenic climate warming that globally may be second only to CO_2 and regionally, such as over East Asia, the dominant driver of climate change. The relative contribution to atmospheric BC from fossil fuel versus biomass combustion is important to constrain as fossil BC is a stronger climate forcer. The source apportionment is the underpinning for targeted mitigation actions. However, technology-based "bottom-up" emission inventories are inconclusive, largely due to uncertain BC emission factors from small-scale/household combustion and open burning. We use "top-down" radiocarbon measurements of atmospheric BC from five sites including three city sites and two regional sites to determine that fossil fuel combustion produces 80 ± 6% of the BC emitted from China. This source-diagnostic radiocarbon signal in the ambient aerosol over East Asia establishes a much larger role for fossil fuel combustion than suggested by all 15 BC emission inventory models, including one with monthly resolution. Our results suggest that current climate modeling should refine both BC emission strength and consider the stronger radiative absorption associated with fossil-fuel-derived BC. To mitigate near-term climate effects and improve air quality in East Asia, activities such as residential coal combustion and city traffic should be targeted.

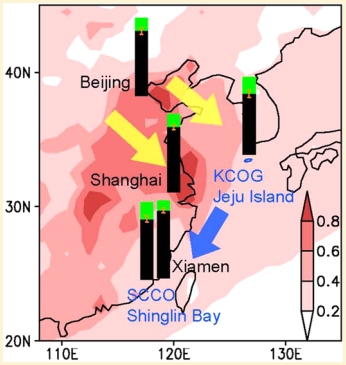

INTRODUCTION

Air pollution, from activities such as residential combustion of coal and wood fuels, traffic, industry, and agricultural burning, contributes gases and particles that combine to form atmospheric brown clouds (ABC), warming the atmosphere yet shading the ground of East and South Asia during winter periods.[1−4] Black carbon (BC)—a comparably large component of Asian ABC—is an important short-lived climate pollutant (SLCP).[1,2,5−10] BC-containing ABC exert a particularly strong influence on climate in East and South Asia, including weakened monsoons,[11,12] intensification of tropical cyclones,[13] tropical expansion,[14] altered rainfall patterns in south and north China,[7,11] and melting of the Himalayan glaciers.[4,15] Furthermore, the health burden of the ABC pollution on individuals and society is large. For example, the estimated premature deaths are of several 100 000s annually in China alone.[2] Accurate information on the relative contribution of BC sources is needed both to efficiently mitigate these multiple effects and to improve description of BC aerosols in climate models.

Emission inventory (EI) models suggest that the tropical-subtropical belt (foremost China and India) contributes 75% of global BC emissions.[2,16] These model estimates are associated with factors of 3−4 uncertainties, and are particularly challenged by highly varying emission factors of BC combustion sources.[16,17] This incomplete understanding of BC sources translates directly into uncertainties also in climate models,[10,18] which are based on these emission inventories. To better constrain the BC sources several assessments call for field-based observations of source-diagnostic tracers to independently evaluate and interactively refine emission inventories.[3,10,16−18] Adding to the urgency to improve on the source constraints, studies show that BC plumes from fossil fuel versus biomass combustion exhibit distinctly different absorption enhancement,[6,19] in part due to effects from

Received: April 12, 2013
Revised: July 6, 2013
Accepted: July 11, 2013
Published: July 11, 2013

coemittants on coating/mixing states and additional scattering, and thus climate warming effects.[20]

To reconcile a previous source dichotomy for BC over South Asia (India and Indian Ocean receptors), the radiocarbon signal (^{14}C) was used as a unique dimension to distinguish the fossil-derived BC (radiocarbon "dead") from biomass-derived BC (radiocarbon "alive").[21] That ^{14}C-based source apportionment suggested ~50% contribution each from fossil fuel and biomass burning for India BC. Given that China is currently the largest BC emitter and the emissions are increasing annually by 4%,[22,23] it is urgent to provide a ^{14}C-based observational determination of BC sources in China. This study reports source-diagnostic ^{14}C dating of aerosol BC[21,24,25] in East Asia with identical sampling methods in three cities spread north–south across eastern China and at two atmospheric observatories serving as regionally integrating background receptors.

MATERIALS AND METHODS

Research Area. Sampling was achieved in three cities spreading north–south across eastern China and at two atmospheric observatories serving as regionally integrating background receptors of East Asia. The densely populated northern-central region of China is the center for heavy urbanization and industrialization and is perennially enveloped by a dense atmospheric brown cloud (ABC) yielding multiple direct and indirect climate and health effects. The dominant atmospheric circulation during the winter season in the study area is driven by the Siberian-Mongolian high-pressure system, which brings cold and dry air southward and eastward (Figure S1 in Supporting Information (SI)).

Rooftop sampling was performed in cities in the north (Beijing), central (Shanghai), and south (Xiamen) of China. Beijing, with 16 million habitants, plays a leading role in the urban clusters of the North China Plain. Shanghai, with 18 million habitants, is a commercial center in the urban clusters of the Yangzi Plain, central China. To obtain a regional apportionment of the sources of the Chinese outflow plume, samples were also collected at the Korea Climate Observatory—Gosan (KCOG, 33.28 N, 126.17 E), Jeju Island in southeast Yellow Sea; and at the South China Climate Observatory (SCCO, 24.61 N, 118.06 E), Shinglin Bay, on the shores of South China Sea.

Aerosol Sampling and Measurement of Black Carbon. Aerosols were collected on precombusted quartz filters mounted on midvolume atmospheric samplers for China sites, and on a high-volume $PM_{2.5}$ sampler for the KCOG high-intensity campaign. The sampling in the three Chinese cities was operated on a daily interval (23 h) during winter 2009–2010. The SCCO sampling ran for the full winter season 2009–2010 dominated by monsoon outflow from north-central China. The KCOG high-volume samples were collected during a two-week high-intensity campaign in March 2011 to investigate air masses from China—The Gosan Pollution Experiment 2011 (GoPoEx11). Additionally, three 7 day samples collected with a lower-volume $PM_{2.5}$ sampler at KCOG from December to late January were utilized to demonstrate that ^{14}C-deduced fossil fraction BC was continuously offset during the entire winter period relative to monthly resolved EI estimates.

For the high-intensity campaigns, 5–9 samples collected during 5–10 days were analyzed for each site (Table S1 in the SI). A 1.5 cm^2 piece of filter was cut out from each sample and analyzed with a thermal-optical transmittance (TOT) carbon analyzer (Sunset Laboratory, Tigard, OR) following the National Institute of Occupational Safety and Health (NIOSH) method 5040 to determine the elemental carbon (EC, as the instrumental proxy for BC) and organic carbon (OC) loadings on the filter.[26] The instrument parameters are adjusted in a sequence so that the first stepped-temperature program in helium (He) atmosphere is followed by a stepped-temperature program executed in 10% oxygen in He. During the analysis, OC was released by thermally volatilizing the particulate carbon on the filter followed by oxidation to carbon dioxide (CO_2) that was simultaneously monitored by a nondispersive infrared detector. Then, the remaining PM on the filter was thermally oxidized to CO_2 to determine the BC. Detailed method descriptions of the Sunset TOT determination of OC and BC concentrations are available in the literature.[27−33] Replicate analyses of sucrose standard and filter samples showed an uncertainty of <10% for OC and BC measurements. Long-term stability of the OC–EC separation was ascertained by stable EC:TC ratios of NIST Reference Material 8785 (urban dust aerosol) as shown in Table S4 in the SI.

Black Carbon Isolation and Analysis of Isotopes. While very similar to our previously reported method,[21] the TOT analyzer was slightly modified to allow for more efficient online isolation of the BC as CO_2 to simplify subsequent preparations for ^{14}C measurements. The CO_2 produced during BC combustion in the TOT analyzer was taken through traps to remove water ($Mg(ClO_4)_2$ anh.) and halogen- and sulfur-containing gases (Ag wool heated to 600 °C) and cryotrapped. The purified CO_2 was then reduced to graphite targets, and the carbon isotopic composition was measured at the U.S. NSF National Ocean Science Accelerator Mass Spectrometry (NOSAMS) facility with due consideration of small-target carbon blank issues.[24,34] $\delta^{13}C$ values are reported as per mil deviation relative to the Vienna Pee Dee Belemnite (VPDB) standard, and radiocarbon analysis results are reported as per mil deviation ($\Delta^{14}C$) relative to NBS oxalic acid I as discussed in detail elsewhere.[24,35]

The putative effect of any potential and inadvertent inclusion of some nonremoved instrument-induced pyrolyzed-C (PyrC, from OC) in the ^{14}C-EC isolate is discussed in SI Materials and Methods and tested in a sensitivity analysis (SI Table S5). The analysis suggests that any effect is likely to be small and in a direction that would elevate the estimated fossil fraction even further and thus act to strengthen the main conclusion. Given the slight modification in protocol for harvesting EC for ^{14}C analysis with the Sunset-TOT instrument between our 2006 India campaign[21] and this study, filters were reanalyzed and the data suggested only a small difference of 2–3% in estimated fossil fraction, which allows comparison between the India and China studies.

Isotope Mass Balance Model. To apportion between the fractional contributions of biomass ($f_{biomass}$) and fossil fuel ($f_{fossil} = 1 - f_{biomass}$) to the BC loading, the natural ^{14}C abundance of BC is expressed in a binary mixing model with the end-members modern biomass and geologically aged radiocarbon-dead fossil fuel.[21,36−39]

$$\Delta^{14}C_{BC} = \Delta^{14}C_{biomass} \times f_{biomass} + \Delta^{14}C_{fossil} \times (1 - f_{biomass}) \quad (1)$$

dx.doi.org/10.1021/es401599r | Environ. Sci. Technol. 2013, 47, 9102–9108

Where $\Delta^{14}C_{BC}$ is measured radiocarbon content of the BC component and $\Delta^{14}C_{fossil}$ is −1000‰. The $\Delta^{14}C$ biomass end member is between +70 and +225‰. The first $\Delta^{14}C$ value (+70‰) corresponds to contemporary CO_2,[40] and thus freshly produced biomass. The second $\Delta^{14}C$ end member (+225‰) is for particles emitted from the combustion of wood,[24,41,42] which has accumulated over the decades-to-century-long life span of trees. The life span of some combusted trees includes the period after the atmospheric nuclear bomb testing that nearly doubled the $\Delta^{14}C$ value of atmospheric CO_2 during the early 1960s. In China, the most important contemporary sources of biomass/biofuel include residential wood fuel and forest fire (161−196 Tg burned wood; SI Table S3), burning of agricultural residue/waste and grassland fires (453−515 Tg burned; freshly produced biomass).[43−46] To regionally parametrize the $\Delta^{14}C_{biomass}$ end member for China as done earlier for India,[21] the average value of 179 Tg wood (27% of total biomass/biofuel) and 484 Tg of freshly produced biomass (73%), were employed. Hence, a China-tailored $\Delta^{14}C_{biomass}$ end member of +112‰ was used in the model calculation. This compares with the estimated India-tailored $\Delta^{14}C_{biomass}$ end member of +199‰, for that region where wood fuel is a relatively more important biomass source. The China end-member selection causes a low sensitive range of ∼3% in the calculated fossil fuel contribution for these East Asia samples (Table 1). A sensitivity test for the choice of the contemporary end member in Table 1 used the extreme/conservative cases of either 100% wood fuel or 100% freshly produced biomass.

Table 1. ^{14}C-Based Source Apportionment between Fossil Fuel and Biomass Combustion for BC Aerosols in East Asia

sites	$f_{biomass}$ (%)	f_{fossil} (%)	full range sensitivity test for average values of f_{fossil} (%)
Beijing	17 ± 4	83 ± 4	82−85
Shanghai	17 ± 4	83 ± 4	82−84
Xiamen	13 ± 3	87 ± 3	87−88
city average	*16 ± 4*	*84 ± 4*	*83−86*
SCCO	22 ± 3	78 ± 4	77−80
KCOG	25 ± 6	75 ± 6	74−77
receptor average	*24 ± 5*	*76 ± 5*	*75−78*
East Asia average	***20 ± 6***	***80 ± 6***	***79−82***

Monthly Resolved Emission Inventory of BC for China from 2008 to 2010. Annual and monthly BC emissions from China by fuel type during 2008−2010 are derived from our previous work.[47] We used a technology-based methodology to estimate the annual BC emissions from China. The emission sources are categorized into five major sectors (i.e., power generation, industry, residential, transport, and open biomass burning) and more than 120 sector/fuel (or product)/technology combinations, including both fuel combustion and noncombustion sources. Time-dependent trends in activity rates and emission factors are incorporated in the calculation.[47] For the seasonal variations of BC emissions, year-specific monthly temporal distributions for each major sector during 2008−2010 were developed. We followed the same methodology used in the TRACE-P (Transport and Chemical Evolution over the Pacific) inventory,[46] assuming a dependence of stove operation on provincial monthly mean temperatures, to generate monthly emissions for the residential sector. For the other sectors, monthly temporal distributions were determined from official biweekly or monthly statistics of power generation, industrial GDP, sulfuric acid and coke production, volume of passenger and freight transported by ship, railway, and aviation, etc. The monthly emissions of open biomass burning from forest and savanna were obtained directly from Global Fire Emissions Database (GFED) version 3.1,[48] and those from agricultural waste burning were determined based on the work of Wang and Zhang.[49]

RESULTS AND DISCUSSION

Black Carbon Pollution from China. BC concentrations were generally high with typical values of 2 $\mu g\ m^{-3}$ in Beijing and Shanghai, 1.5 $\mu g\ m^{-3}$ at the South China Climate Observatory (SCCO) and 0.8 $\mu g\ m^{-3}$ at the Korea Climate Observatory—Gosan (KCOG) (Figure 2A). Beijing and Shanghai are two megacities of East Asia, which, particularly in wintertime, experience widespread and concentrated ABC as indicated by high average values of satellite-derived aerosol optical depth (AOD; Figure 1). The thick ABC shading of the densely populated northern-central region of China[50,51] yields multiple direct and indirect climate effects in Asia.[1,4,11,19,52,53] AOD (Figure 1), in combination with analysis of atmospheric circulation (SI Figure S1) and receptor-oriented air trajectories (SI Figure S2), suggests that the dispersion of this ABC outflow plume from northern-central China predominantly follows a coastline pathway during the December−March study period, and influences large areas in East/Southeast Asia. The lower BC concentrations at KCOG (0.77 ± 0.36 $\mu g\ m^{-3}$) and SCCO (1.46 ± 0.48 $\mu g\ m^{-3}$) than in the three urban areas (2.16 ± 0.62 $\mu g\ m^{-3}$) is consistent with these two receptor sites being able to provide a regionally integrated picture of the BC-containing ABC plume from China. Taken together, our sampling at the downwind sites KCOG and SCCO thus successfully intercepted the heavy air pollution events associated with the Chinese outflow plume (SI Figure S2).

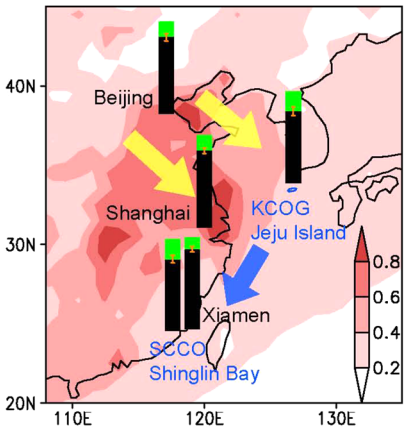

Figure 1. Satellite-derived distribution of the ABC over East Asia with locations of sampling sites and ^{14}C-based apportionment of BC sources. ABC coverage (contour shading) is traced by AOD at 550 nm (average for years 2008−2011). The thick arrows indicate the prevailing pathway of Asian winter monsoon outflow projected from meteorological modeling for 1948−2011 (SI Figure S1) and backward trajectories (SI Figure S2) during the months of the sampling campaigns. The base of the inserted bars indicates locations of the five sampling sites. The bar color fill indicates ^{14}C-based estimate of contribution to the BC from combustion of fossil fuel (black) and biomass (green).

dx.doi.org/10.1021/es401599r | Environ. Sci. Technol. 2013, 47, 9102−9108

Radiocarbon-Based Source Apportionment of BC. The BC isolates exhibited both temporal and geographical uniformity in radiocarbon signal, yielding narrow constraints on the contributions to BC from fossil versus biomass combustion sources in China. The full ranges of the Δ^{14}C-BC signal (Figure 2B) measured at the five sites were −892 ± 12‰ to −627 ± 4‰ (n = 37: SI Table S1). Slightly more depleted Δ^{14}C values were recorded for the cities, with near-identical values of Δ^{14}C in Beijing (−813 ± 46‰, 1SD; n = 6) and Shanghai (−807 ± 40‰; n = 7). This signals a clear predominance of fossil-fuel combustion as a source of wintertime BC in northern-central China. Dual-isotope probing, combining Δ^{14}C with δ^{13}C (SI Figure S3), is consistent with fossil fuel combustion being the predominant source, yet the end members for δ^{13}C are less well constrained. However, the δ^{13}C-EC values signal that coal usage may be a relatively more important fossil source in Beijing in north China whereas fossil emissions from traffic may be relatively more important for the region of Shanghai in central China. The somewhat less depleted values of Δ^{14}C at the regional receptor sites KCOG (−727 ± 68‰; n = 12) and SCCO (−754 ± 42‰; n = 7) indicate a somewhat higher contribution of biomass burning in rural areas than from China megacities. Three samples at the KCOG site with lowest Δ^{14}C values (<−800‰; SI Table S1) were associated with air masses from the densely populated northern-central China (SI Figure S2; KCOG4, KCOG7, and KCOG8), whereas those samples influenced largely by air mass from rural mountains and plateaus in northern China showed relatively less depleted ^{14}C. The ubiquitous use of raw coal and coal briquettes in small domestic stoves, cookers, and heaters have few or insufficient emission controls in densely populated northern-central China where coal is in abundant supply.[45,54,55] The relative depletion of δ^{13}C in KCOG compared to the other sites may be reflecting that the KCOG campaign was performed at the end of winter when domestic coal usage for heating in N. China had likely declined some. Taken together, the key culprits responsible for BC pollution over East Asia appear to be fossil-fuel combustion such as small-scale coal combustion and vehicle emissions in these densely populated and urbanized areas of the north-central corridor of eastern China.

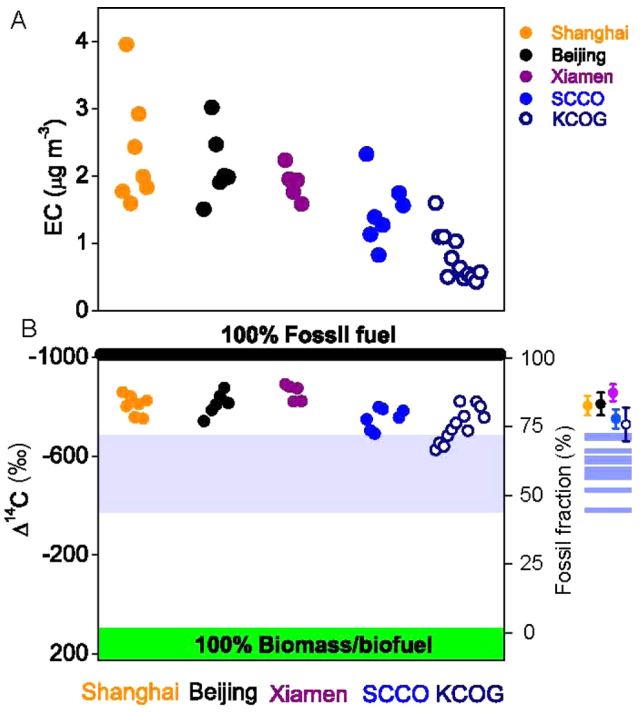

Figure 2. Wintertime concentration and ^{14}C-based source apportionment of BC aerosols over East Asia. (A) Mass-based ~24 h BC concentrations at the five sites; (B) Radiocarbon signal (Δ^{14}C) of BC aerosols. The Δ^{14}C end-member ranges are shown for both contemporary biomass/biofuel (lower green field) and for fossil fuel combustion (upper thick black line). The fossil fuel contribution constrained from ambient Δ^{14}C-based measurements (points; this study) are compared with estimates from 15 emission inventories (blue lines in the right column of panel B; SI Table S2) with their full range also shown as a blue transparent field inside the figure.

Difference between "Bottom-Up" and "Top-Down" Estimates. To afford a detailed comparison with "bottom-up" estimates of BC emission and earlier "top-down" BC source apportionment studies, a simple isotope mass balance equation[21] based on Δ^{14}C was applied to apportion between the fractional contributions of biomass ($f_{biomass}$) and fossil fuel ($f_{fossil} = 1 - f_{biomass}$) combustion to BC from China (Materials and Methods). Application of the isotope mass balance model to the Chinese Δ^{14}C-BC values revealed contribution from fossil fuel combustion of 84 ± 4% in cities and 76 ± 5% in regional receptor sites (Table 1). These ^{14}C-based constraints indicate an overall larger role of fossil fuel combustion for China BC (80 ± 6%), compared to the estimates of 15 emission inventories (61 ± 7%; SI Table S2). These source-resolved EI estimates are reported in the literature only as annual averages. The one EI study with monthly resolution suggested an even lower contribution (55 ± 1%) of fossil-fuel combustion to BC in the winter (corresponding to the period of the ^{14}C-BC field campaigns) than the annual average, yielding an even larger offset between bottom-up EI models and top-down ^{14}C-BC measurements (Figure 3). Interestingly, the fossil-fuel fraction of BC estimated by emission inventory models is lower than the apportionment based on the ambient ^{14}C-BC signal in both China and India (Figure 4). This indicates that there could be either a systematic model overestimation of BC emissions from biomass burning or underestimation of BC emissions from fossil-fuel combustion

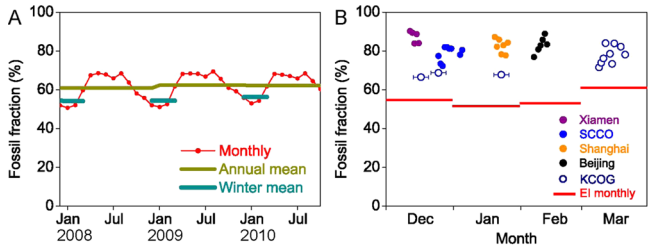

Figure 3. Temporal information for both "bottom-up" emission inventory (EI) model and "top-down" ^{14}C-based atmospheric measurements for fraction of fossil BC from China. (A) Monthly variation of fossil fraction BC from emission inventory for 2008−2010. Winter mean is the average of Dec, Jan, Feb and Mar, which is the main season for BC emissions (45 ± 1% of annual BC emissions) and corresponds to the period of the East Asia ^{14}C-BC field campaigns. (B) Comparison between EI and ^{14}C-based sourcing of fossil fraction BC for the winter months. The horizontal bars for the three KCOG samples taken during December to late January indicate the 7 day sampling durations, whereas other data points have sampling durations of about one day.

dx.doi.org/10.1021/es401599r | Environ. Sci. Technol. 2013, 47, 9102−9108

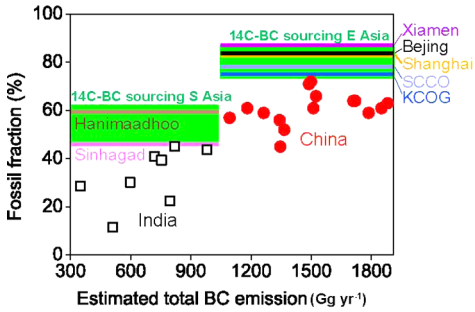

Figure 4. Comparison of fossil fraction of atmospheric BC based on ^{14}C measurements of ambient aerosols (green fields) and estimates from emission inventory models (squares and circles), as a function of the model-estimated total BC emissions for China and India. The thickness of the green fields indicates 1 SD of the ^{14}C-based apportionment of the fossil fuel contribution with average values for individual locations indicated as horizontal lines. The 15 emission inventory models are detailed in SI Table S2.

such as for the uncontrolled coal usage for domestic heating and cooking[17,54] and high-emitting vehicles with malfunctioning engines (black smokers),[16] or both. Several other "top-down" studies at a few locations inside China, while providing less quantitative constraints on the fossil vs biomass contributions than the direct ^{14}C-based "dating" of the atmospheric BC, also suggest a possible underestimation of the relative contribution to BC emissions from fossil fuel combustion in China by EI models.[56,57] Further indirect evidence from recent climate modeling shows that a larger emission of BC than current inventory estimates from Asia is required to better simulate the climate change in tropical-subtropical areas.[10,14,20]

Co-Benefits of BC Mitigation in China. A relatively larger role for fossil-fuel derived BC also has implications pertaining to climate forcing. It has been reported that fossil-fuel-dominated BC plumes are approximately 100% more efficient warming agents than biomass-burning-dominated BC plumes because biomass burning coemits a larger fraction of radiation-scattering OC, whereas coating enhancement of BC absorption may be stronger in fossil-fuel dominated plumes.[6,19] Current climate models may hence underestimate the BC warming effect due to both emissions and stronger warming/forcing of fossil-fuel derived BC plumes. A relatively larger contribution of fossil-fuel derived BC to the total BC loading over Asia than currently parameterized in climate models (BC loadings are based on the emission inventories) may in part help to resolve the relatively lower BC climate forcing in models (0.05−0.55 W m^{-2})[5,14] than estimated from ambient atmospheric solar heating measurements, satellite and ground-network observations (0.9−1.2 W m^{-2}).[1,20,58] Hence, these isotope-based BC source constraints tend to increase the potential benefit, in terms of decreased climate forcing, by mitigating BC emissions from fossil fuel sources in China. The current results suggest reduction measures in China should focus on domestic coal combustion (e.g., introduction of cleaner-burning cookers and heaters) and vehicle emissions (e.g., application of diesel particle filters[2]). Such mitigation efforts have the potential over the coming years-decades to improve air quality with multiple cobenefits including improved human health (an estimated annual avoidance of nearly 700 000 premature deaths for China by 2030) and reduced anthropogenic climate forcing over vast areas of Asia.[2,6,10]

■ ASSOCIATED CONTENT

Supporting Information

Sensitivity analysis of EC isolation, figures describing winter monsoon, backward trajectory analysis during sampling season, $\delta^{13}C$ and $\Delta^{14}C$ relationship for BC from Beijing and Shanghai, as well as tables listing original data of ^{14}C analysis and summary of fossil and total BC emissions from emission inventory models are provided. This material is available free of charge via the Internet at http://pubs.acs.org.

■ AUTHOR INFORMATION

Corresponding Author

*Phone: +86-592-6190767 (K.D.); +46-70-347317 (Ö.G.). E-mail: kdu@iue.ac.cn (K.D.); orjan.gustafsson@itm.su.se (Ö.G.).

Present Address

○B.C.: Environmental Research Institute, Shandong University, Jinan 250100, China.

Notes

The authors declare no competing financial interest.

■ ACKNOWLEDGMENTS

The research was financially supported by the Swedish funding agencies FORMAS (Nr. 214-2009-970) and STINT (Nr. 2010/072), the National Natural Science Foundation of China (Nr. 40905065) the Knowledge Innovation Program of the Chinese Academy of Sciences (Nr. KZCX2-EW-408) and the Korean Center for Atmospheric and Earthquake Research. Argonne National Laboratory acknowledges the support of NASA's Modeling, Analysis and Predictability (MAP) program. Ö.G. additionally acknowledges support as an Academy Research Fellow at the Swedish Royal Academy of Sciences through a grant from the Knut and Alice Wallenberg Foundation and B.C. the Independent Innovation Foundation of Shandong University (Nr. 2013TB003).

■ REFERENCES

(1) Ramanathan, V.; Carmichael, G. Global and regional climate changes due to black carbon. *Nat. Geosci.* **2008**, *1*, 221−227.

(2) Shindell, D.; Kuylenstierna, J. C. I.; Vignati, E.; Dingenen, R. v.; Amann, M.; Klimont, Z.; Anenberg, S. C.; Muller, N.; Janssens-Maenhout, G.; Raes, F.; Schwartz, J.; Faluvegi, G.; Pozzoli, L.; Kupiainen, K.; Höglund-Isaksson, L.; Emberson, L.; Streets, D. G.; Ramanathan, V.; Hicks, K.; Oanh, N. T. K.; Milly, G.; Williams, M.; Demkine, V.; Fowler, D. Simultaneously mitigating near-term climate change and improving human health and food security. *Science* **2012**, *335*, 183−189.

(3) Lawrence, M. G.; Lelieveld, J. Atmospheric pollutant outflow from southern Asia: A review. *Atmos. Chem. Phys.* **2010**, *10*, 11017−11096.

(4) Ramanathan, V.; Ramana, M. V.; Roberts, G.; Kim, D.; Corrigan, C.; Chung, C.; Winker, D. Warming trends in Asia amplified by brown cloud solar absorption. *Nature* **2007**, *448*, 575−578.

(5) Forster, P.; Ramaswamy, V.; Artaxo, P.; Berntsen, T.; Betts, R.; Fahey, D. W.; Haywood, J.; Lean, J.; Lowe, D. C.; Myhre, G.; Nganga, J.; Prinn, R.; ; Raga, G.; Schulz, M.; Dorland, R. V. In *Climate Change 2007: The Physical Science Basis. Contribution of Working Group I to the Fourth Assessment Report of the Intergovernmental Panel on Climate Change*; Solomon, S., Qin, D., Manning, M., Chen, Z., Marquis, M., Averyt, K. B., Tignor, M., Miller, H. L., Eds.; Cambridge University Press: Cambridge, 2007.

(6) Jacobson, M. Z. Shot-term effects of controlling fossil-fuel soot, biofuel soot and gases, and methane on climate, Arctic ice, and air pollution health. *J. Geophys. Res.* **2010**, *115*, D14209.

(7) Ramanathan, V.; Chung, C.; Kim, D.; Bettge, T.; Buja, L.; Kiehl, J. T.; Washington, W. M.; Fu, Q.; Sikka, D. R.; Wild, M. Atmospheric brown clouds: Impacts on South Asian climate and hydrological cycle. *Proc. Natl. Acad. Sci. U.S.A.* **2005**, *102*, 5326−5333.
(8) Lack, D. A.; Langridge, J. M.; Bahreini, R.; Cappa, C. D.; Middlebrook, A. M.; Schwarz, J. P. Brown carbon and internal mixing in biomass burning particles. *Proc. Natl. Acad. Sci. U.S.A.* **2012**, *109*, 14802−14807.
(9) Moffet, R. C.; Prather, K. A. In-situ measurements of the mixing state and optical properties of soot with implications for radiative forcing estimates. *Proc. Natl. Acad. Sci. U.S.A.* **2009**, *106*, 11872−11877.
(10) Bond, T. C.; Doherty, S. J.; Fahey, D. W.; Forster, P. M.; Berntsen, T.; DeAngelo, B. J.; Flanner, M. G.; Ghan, S.; Kärcher, B.; Koch, D.; Kinne, S.; Kondo, Y.; Quinn, P. K.; Sarofim, M. C.; Schultz, M. G.; Schulz, M.; Venkataraman, C.; Zhang, H.; Zhang, S.; Bellouin, N.; Guttikunda, S. K.; Hopke, P. K.; Jacobson, M. Z.; Kaiser, J. W.; Klimont, Z.; Lohmann, U.; Schwarz, J. P.; Shindell, D.; Storelvmo, T.; Warren, S. G.; Zender, C. S. Bounding the role of black carbon in the climate system: A scientific assessment. *J. Geophys. Res. Atmos.* **2013**, DOI: 10.1002/jgrd.50171.
(11) Menon, S.; Hansen, J.; Nazarenko, L.; Luo, Y. Climate effects of black carbon aerosols in China and India. *Science* **2002**, *297*, 2250−2253.
(12) Bollasina, M. A.; Ming, Y.; Ramaswamy, V. Anthropogenic aerosols and the weakening of the South Asian summer monsoon. *Science* **2011**, *334*, 502−505.
(13) Evan, A. T.; Kossin, J. P.; Eddy, C. C.; Ramanathan, V. Arabian Sea tropical cyclones intensified by emissions of black carbon and other aerosols. *Nature* **2011**, *479*, 94−97.
(14) Allen, R. J.; Sherwood, S. C.; Norris, J. R.; Zender, C. S. Recent Northern Hemisphere tropical expansion primarily driven by black carbon and tropospheric ozone. *Nature* **2012**, *485*, 350−354.
(15) Xu, B.; Cao, J.; Hansen, J.; Yao, T.; Joswia, D. R.; Wang, N.; Wu, G.; Wang, M.; Zhao, H.; Yang, W.; Liu, X.; He, J. Black soot and the survival of Tibetan glaciers. *Proc. Natl. Acad. Sci. U.S.A.* **2009**, *106*, 22114−22118.
(16) Bond, T. C.; Streets, D. G.; Yarber, K. F.; Nelson, S. M.; Woo, J.-H.; Klimont, Z. A technology-based global inventory of black and organic carbon emissions from combustion. *J. Geophys. Res.* **2004**, *109*, D14203.
(17) Zhao, Y.; Nielsen, C. P.; Lei, Y.; McElroy, M. B.; Hao, J. Quantifying the uncertainties of a bottom-up emission inventory of anthropogenic atmospheric pollutants in China. *Atmos. Chem. Phys.* **2011**, *11*, 2295−2308.
(18) Menon, S.; Koch, D.; Beig, G.; Sahu, S.; Fasullo, J.; Orlikowski, D. Black carbon aerosols and the third polar ice cap. *Atmos. Chem. Phys.* **2010**, *10*, 4559−4571.
(19) Ramana, M. V.; Ramanathan, V.; Feng, Y.; Yoon, S.-C.; Kim, S.-W.; Carmichael, G. R.; Schauer, J. J. Warming influenced by the ratio of black carbon to sulphate and the black-carbon source. *Nat. Geosci.* **2010**, *3*, 542−545.
(20) Chung, C. E.; Ramanathan, V.; Decremer, D. Observationally constrained estimates of carbonaceous aerosol radiative forcing. *Proc. Natl. Acad. Sci. U.S.A.* **2012**, *109*, 11624−11629.
(21) Gustafsson, Ö.; Kruså, M.; Zencak, Z.; Sheesley, R. J.; Granat, L.; Engström, E.; Praveen, P. S.; Rao, P. S. P.; Leck, C.; Rodhe, H. Brown clouds over South Asia: Biomass or fossil fuel combustion? *Science* **2009**, *323*, 495−498.
(22) Lu, Z.; Zhang, Q.; Streets, D. G. Sulfur dioxide and primary carbonaceous aerosol emissions in China and India, 1996−2010. *Atmos. Chem. Phys.* **2011**, *11*, 9839−9864.
(23) Qin, Y.; Xie, S. D. Spatial and temporal variation of anthropogenic black carbon emissions in China for the period 1980−2009. *Atmos. Chem. Phys.* **2012**, *12*, 4825−4841.
(24) Zencak, Z.; Elmquist, M.; Gustafsson, Ö. Quantification and radiocarbon source apportionment of black carbon in atmospheric aerosols using the CTO-375 method. *Atmos. Environ.* **2007**, *41*, 7895−7906.
(25) Zencak, Z.; Reddy, C. M.; Teuten, E. L.; Xu, L.; McNichol, A. P.; Gustafsson, Ö. Evaluation of gas chromatographic isotope fractionation and process contamination by carbon in compound-specific radiocarbon analysis. *Anal. Chem.* **2007**, *79*, 2042−2049.
(26) Birch, M. E.; Cary, R. A. Elemental carbon-based method for occupational monitoring of particulate diesel exhaust: Methodology and exposure issues. *Analyst* **1996**, *121*, 1183−1190.
(27) Arhami, M.; Kuhn, T.; Fine, P. M.; Delfino, R. J.; Sioutas, C. Effects of sampling artifacts and operating parameters on the performance of a semicontinuous particulate elemental carbon/organic carbon monitor. *Environ. Sci. Technol.* **2005**, *40*, 945−954.
(28) Bae, M.-S.; Schauer, J. J.; DeMinter, J. T.; Turner, J. R.; Smith, D.; Cary, R. A. Validation of a semi-continuous instrument for elemental carbon and organic carbon using a thermal-optical method. *Atmos. Environ.* **2004**, *38*, 2885−2893.
(29) Bauer, J. J.; Yu, X.-Y.; Cary, R.; Laulainen, N. S.; Berkowitz, C. M. Characterization of the sunset semi-continuous carbon aerosol analyzer. *J. Air Waste Manage. Assoc.* **2009**, *59*, 826−833.
(30) Lim, H.-J.; Turpin, B. J.; Edgerton, E.; Hering, S. V.; Allen, G.; Maring, H.; Solomon, P. Semicontinuous aerosol carbon measurements: Comparison of Atlanta Supersite measurements. *J. Geophys. Res.* **2003**, *108*, 8419.
(31) Rice, J. Comparison of integrated filter and automated carbon aerosol measurements at Research Triangle Park, North Carolina. *Aerosol Sci. Technol.* **2004**, *38*, 23−36.
(32) Yang, H.; Yu, J. Z. Uncertainties in charring correction in the analysis of elemental and organic carbon in atmospheric particles by thermal/optical methods. *Environ. Sci. Technol.* **2002**, *36*, 5199−5204.
(33) Jeong, C.-H.; Hopke, P. K.; Kim, E.; Lee, D.-W. The comparison between thermal-optical transmittance elemental carbon and Aethalometer black carbon measured at multiple monitoring sites. *Atmos. Environ.* **2004**, *38*, 5193−5204.
(34) Pearson, A.; McNichol, A. P.; Schneider, R. J.; Von, R. F.; Zheng, Y. Microscale AMS 14C measurement at NOSAMS. *Radiocarbon* **1998**, *40*, 61−75.
(35) Stuiver, M.; Polach, H. A. Reporting of C-14 data—Discussion. *Radiocarbon* **1977**, *19*, 355−363.
(36) Aiken, A. C.; Foy, B. d.; Wiedinmyer, C.; DeCarlo, P. F.; Ulbrich, I. M.; Wehrli, M. N.; Szidat, S.; Prevot, A. S. H.; Noda, J.; Wacker, L.; Volkamer, R.; Fortner, E.; Wang, J.; Laskin, A.; Shutthanandan, V.; Zheng, J.; Zhang, R.; Paredes-Miranda, G.; Arnott, W. P.; Molina, L. T.; Sosa, G.; Querol, X.; Jimenez, J. L. Mexico city aerosol analysis during MILAGRO using high resolution aerosol mass spectrometry at the urban supersite (T0)—Part 2: Analysis of the biomass burning contribution and the non-fossil carbon fraction. *Atmos. Chem. Phys.* **2010**, *10*, 5315−5341.
(37) Uchida, M.; Kumata, H.; Koike, Y.; Tsuzuki, M.; Uchida, T.; Fujiwara, K.; Shibata, Y. Radiocarbon-based source apportionment of black carbon (BC) in PM10 aerosols from residential area of suburban Tokyo. *Nucl. Instrum. Methods Phys. Res., Sect. B* **2010**, *268*, 1120−1124.
(38) Heal, M. R.; Naysmith, P.; Cook, G. T.; Xu, S.; Duran, T. R.; Harrison, R. M. Application of 14C analyses to source apportionment of carbonaceous PM2.5 in the UK. *Atmos. Environ.* **2011**, *45*, 2341−2348.
(39) Handa, D.; Nakajima, H.; Arakaki, T.; Kumata, H.; Shibata, Y.; Uchidac, M. Radiocarbon analysis of BC and OC in PM_{10} aerosols at Cape Hedo, Okinawa, Japan, during long-range transport events from East Asian countries. *Nucl. Instrum. Methods Phys. Res., Sect. B* **2010**, *268*, 1125−1128.
(40) Levin, I.; Kromer, B.; Schmidt, M.; Sartorius, H. A novel approach for independent budgeting of fossil fuel CO_2 over Europe by $14CO_2$ observations. *Geophys. Res. Lett.* **2003**, *30*, 2194.
(41) Szidat, S.; Prévôt, A. S. H.; Sandradewi, J.; Alfarra, M. R.; Synal, H.-A.; Wacker, L.; Baltensperger, U. Dominant impact of residential wood burning on particulate matter in Alpine valleys during winter. *Geophys. Res. Lett.* **2007**, *34*, L05280.

(42) Klinedinst, D. B.; Currie, L. A. Direct Quantification of $PM_{2.5}$ fossil and biomass carbon within the northern front range air quality study's domain. *Environ. Sci. Technol.* **1999**, *33*, 4146−4154.
(43) Zhang, Q.; Streets, D. G.; He, K.; Klimont, Z. Major components of China's anthropogenic primary particulate emissions. *Environ. Res. Lett.* **2007**, *2*, 045027.
(44) NBS; China Statistics Press: Beijing, 2004.
(45) Cao, G.; Zhang, X.; Zheng, F. Inventory of black carbon and organic carbon emissions from China. *Atmos. Environ.* **2006**, *40*, 6516−6527.
(46) Streets, D. G.; Bond, T. C.; Carmichael, G. R.; Fernandes, S. D.; Fu, Q.; He, D.; Klimont, Z.; Nelson, S. M.; Tsai, N. Y.; Wang, M. Q.; Woo, J. H.; Yarber, K. F. An inventory of gaseous and primary aerosol emissions in Asia in the year 2000. *J. Geophys. Res.* **2003**, *108*, 8809.
(47) Lu, Z.; Zhang, Q.; Streets, D. G. Sulfur dioxide and primary carbonaceous aerosol emissions in China and India, 1996−2010. *Atmos. Chem. Phys.* **2011**, *11*, 9839−9864.
(48) van der Werf, G. R.; Randerson, J. T.; Giglio, L.; Collatz, G. J.; Mu, M.; Kasibhatla, P. S.; Morton, D. C.; DeFries, R. S.; Jin, Y.; van Leeuwen, T. T. Global fire emissions and the contribution of deforestation, savanna, forest, agricultural, and peat fires (1997−2009). *Atmos. Chem. Phys.* **2010**, *10*, 11707−11735.
(49) Wang, S.; Zhang, C. Spatial and temporal distribution of air pollutant emissions from open burning of crop residues in China. *Science Paper Online (in Chinese)* **2008**, *3*, 329−333.
(50) Yang, X.; Hou, Y.; Chen, B. Observed surface warming induced by urbanization in east China. *J. Geophys. Res.* **2011**, *116*, D14113.
(51) Bloom, D. E. 7 Billion and Counting. *Science* **2011**, *333*, 562−569.
(52) Alexander, D. T. L.; Crozier, P. A.; Anderson, J. R. Brown carbon spheres in East Asian outflow and their optical properties. *Science* **2008**, *321*, 833−836.
(53) Kaufman, Y. J.; Tanre, D.; Boucher, O. A satellite view of aerosols in the climate system. *Nature* **2002**, *419*, 215−223.
(54) Zhang, Q.; Streets, D. G.; Carmichael, G. R.; He, K. B.; Huo, H.; Kannari, A.; Klimont, Z.; Park, I. S.; Reddy, S.; Fu, J. S.; Chen, D.; Duan, L.; Lei, Y.; Wang, L. T.; Yao, Z. L. Asian emissions in 2006 for the NASA INTEX-B mission. *Atmos. Chem. Phys.* **2009**, *9*, 5131−5153.
(55) Zhang, Q.; He, K. B.; Huo, H. Cleaning China's air. *Nature* **2012**, *484*, 161−162.
(56) Wang, Y.; Wang, X.; Kondo, Y.; Kajino, M.; Munger, J. W.; Hao, J. Black carbon and its correlation with trace gases at a rural site in Beijing: Top-down constraints from ambient measurements on bottom-up emissions. *J. Geophys. Res.* **2011**, *116*, D24304.
(57) Fu, T.-M.; Cao, J. J.; Zhang, X. Y.; Lee, S. C.; Zhang, Q.; Han, Y. M.; Qu, W. J.; Han, Z.; Zhang, R.; Wang, Y. X.; Chen, D.; Henze, D. K. Carbonaceous aerosols in China: Top-down constraints on primary sources and estimation of secondary contribution. *Atmos. Chem. Phys.* **2012**, *12*, 2725−2746.
(58) Sato, M.; Hansen, J.; Koch, D.; Lacis, A.; Ruedy, R.; Dubovik, O.; Holben, B.; Chin, M.; Novakov, T. Global atmospheric black carbon inferred from AERONET. *Proc. Natl. Acad. Sci. U.S.A.* **2003**, *100*, 6319−6324.